Thermal Dosimetry Predictive of Efficacy of ^{111}In-ChL6 Nanoparticle AMF–Induced Thermoablative Therapy for Human Breast Cancer in Mice

Sally J. DeNardo[1], Gerald L. DeNardo[1], Arutselvan Natarajan[1], Laird A. Miers[1], Allan R. Foreman[2], Cordula Gruettner[3], Grete N. Adamson[1], and Robert Ivkov[2]

[1]School of Medicine, University of California Davis, Sacramento, California; [2]Triton BioSystems, Inc., Chelmsford, Massachusetts; and [3]Micromod Partikeltechnologie, GmbH, Rostock-Warnemuende, Germany

Antibody (mAb)-linked iron oxide nanoparticles (bioprobes) provide the opportunity to develop tumor specific thermal therapy (Rx) for metastatic cancer when inductively heated by an externally applied alternating magnetic field (AMF). To evaluate the potential of this Rx, in vivo tumor targeting, efficacy, and predictive radionuclide-based heat dosimetry were studied using ^{111}In-ChL6 bioprobes (ChL6 is chimeric L6) in a human breast cancer xenograft model. **Methods:** Using carbodiimide, ^{111}In-DOTA-ChL6 (DOTA is dodecanetetraacetic acid) was conjugated to polyethylene glycol-iron oxide–impregnated dextran 20-nm particles and purified as ^{111}In-bioprobes. [111]In doses of 740–1,110 kBq (20–30 μCi) (2.2 mg of bioprobes) were injected intravenously into mice bearing HBT3477 human breast cancer xenografts. Pharmacokinetic (PK) data were obtained at 1, 2, 3, and 5 d. AMF was delivered 72 h after bioprobe injection at amplitudes of 1,410 (113 kA/m), 1,300 (104 kA/m), and 700 (56 kA/m) oersteds (Oe) at 30%, 60%, and 90% "on" time (duty), respectively, and at 1,050 Oe (84 kA/m) at 50% and 70% duty over the 20-min treatment. Treated and control mice were monitored for 90 d. Tumor total heat dose (THD) from activated tumor bioprobes was calculated for each Rx group using ^{111}In-bioprobe tumor concentration and premeasured particle heat response to AMF amplitudes. Tumor growth delay was analyzed by Wilcoxon rank sum comparison of time to double, triple, and quintuple tumor volume in each group, and all groups were compared with the controls. **Results:** Mean tumor concentration of ^{111}In-bioprobes at 48 h was 14 ± 2 percentage injected dose per gram; this concentration 24 h before AMF treatment was used to calculate THD. No particle-related toxicity was observed. Toxicity was observed at the highest AMF amplitude–duty combination of 1,300 Oe and 60% over 20 min; 6 of 10 mice died acutely. Tumor growth delay occurred in all of the other groups, correlated with heat dose and, except for the lowest heat dose group, was statistically significant when compared with the untreated group. Electron microscopy showed ^{111}In-bioprobes on tumor cells and cell death by necrosis at 24 and 48 h after AMF. **Conclusion:** mAb-guided bioprobes (iron oxide nanoparticles) effectively targeted human breast cancer xenografts in mice. THD, calculated using empirically observed ^{111}In-bioprobe tumor concentration and in vitro nanoparticle heat induction by AMF, correlated with tumor growth delay.

Key Words: monoclonal antibodies; nanoparticle; alternating magnetic fields; thermoablation; cancer

J Nucl Med 2007; 48:437–444

The potential of hyperthermia and thermal ablation in cancer therapy has been well noted (1–5). Temperatures between 42°C and 46°C lead to inactivation of normal cellular processes, whereas above 46°C, extensive necrosis occurs. However, the inability to deposit effective doses of heat in tumor without applying similar heat to nearby normal tissue has prevented widespread clinical use. Difficulties in predicting thermal dose, or obtaining accurate in situ measurements, have been additional problems. New technology is needed to deliver heat selectively to tumor cells and provide predictive dosimetry.

Nanoparticles that are responsive to alternating magnetic frequency (AMF), when conjugated with antitumor monoclonal antibodies (mAb), provide a new approach to direct thermal ablation specifically to tumor cells. Given systemically, such mAb-linked nanoparticles (bioprobes) can reach and bind to tumor cells. If levels of AMF that are not toxic to normal tissues can be applied from an external source to instantaneously heat bioprobes in tumor tissues above 46°C, then selective thermal ablation of tumor cells with little effect on the normal tissues should be possible.

Measuring heat in the tumor cell microenvironment, though not affecting the biologic response under study, is not achievable with standard technology. However, calculations of the total heat dose (THD) created by a given AMF amplitude per unit time can be obtained using the measured heat response of the bioprobes in vitro and concentration of bioprobes in vivo. Although this does

not provide information on bystander tissue heating or eddy current production, or the degree of homogeneity in tumor, it allows comparison of tumor response with the calculated THD (joules).

This study presents evidence that this approach is realistic and that the joules of heat predicted in tumor relate to response. Tumor uptake of ^{111}In-bioprobes and evidence of tumor responses after AMF application were observed in our initial studies in mice (6). These preliminary results led to the current study plan in which AMF treatment groups given 90-s AMF pulses in a 20-min treatment period allowed more critical evaluation of response and toxicity. In this article we describe the radiolabeled mAb conjugation with 20-nm nanoparticles to produce tumor-binding ^{111}In-bioprobes (Fig. 1): the pharmacokinetics (PK) in human tumor xenografted mice, in vivo tumor targeting, and tumor response to bioprobe/AMF therapy (Rx). Efficacy is compared with the calculated heat achieved by AMF amplitudes applied to mice with bioprobes in tumor tissue. Temporal progression of tumor necrosis after Rx is documented by electron microscopy (EM) of excised tumors.

MATERIALS AND METHODS

Carrier-free [111]In (MDS Nordion) was purchased as chloride in 0.05 mol/L HCl. Chimeric L6 (ChL6), human–mouse mAb chimera (Bristol-Myers Squibb Pharmaceutical Research Institute), reacts with an integral membrane glycoprotein highly expressed on human breast, colon, ovary, and lung carcinomas
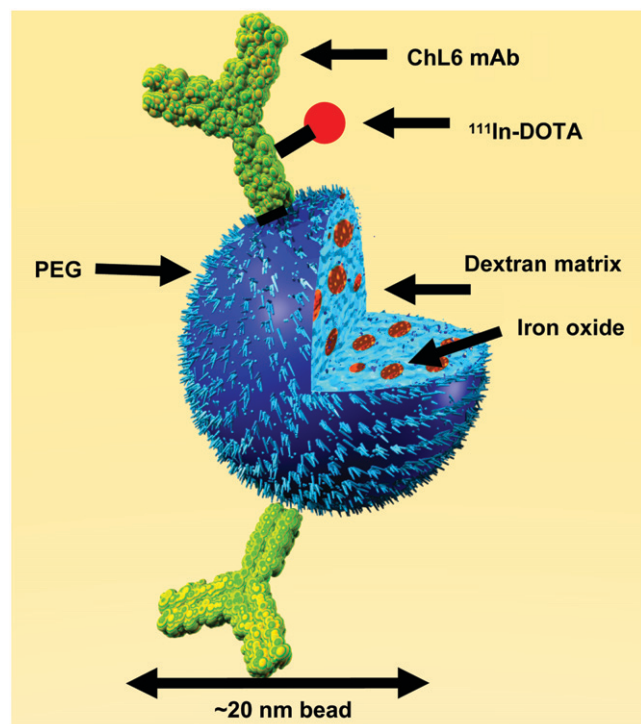
FIGURE 1. Schematic of a bioprobe: ^{111}In-ChL6 conjugated to PEG on iron oxide–impregnated dextran 20-nm nanoparticles.

(7–10). ChL6 was specified as >95% pure monomeric IgG by polyacrylamide gel electrophoresis.

High-gradient magnetic field (HGMF) columns and Nanomag-D-Spio 20-nm (Spio = superparamagnetic iron oxide) (polyethylene glycol [PEG]-coated iron oxide–impregnated dextran) beads in suspension (17 mg/mL; 6.5 mg Fe/mL) were obtained from Micromod Partikeltechnologie, GmbH. 2-(4-Morpholino)ethanesulfonic acid (MES), 1-ethyl-3-(3-dimethylaminopropyl)carbodiimide HCl (EDC), N-hydroxysuccinimide (NHS), glycine, 2-iminothiolane (2IT), and phosphate-buffered saline ([PBS] Sigma Chemical Co.) and 3,400 molecular-weight cutoff (MWCO) dialysis bags (Pierce Chemicals) were purchased.

Conjugation of ChL6 with 2-[p-bromoacetamido) benzyl]-DOTA (DOTA Is Dodecanetetraacetic Acid)

The immunoconjugate, 2IT-BAD-ChL6, was prepared by conjugating 2-[p-(bromoacetamido)benzyl]-1,4,7,10-tetraazacyclodo-decane-N,N',N'',N'''-tetraacetic acid DOTA (BAD) to ChL6 via 2IT as previously described (11). Final concentrations of 2.0 mmol/L BAD, 15 mg/mL ChL6, and 1.3 mmol/L 2IT were used in 0.1 mol/L tetramethylammonium phosphate, pH 9, at 37°C with 30-min incubation. The 2IT-BAD-ChL6 conjugate was purified and transferred to 0.1 mol/L ammonium acetate, pH 5.3, by G50 molecular-sieving chromatography. A mean of 1.3 DOTA groups was conjugated per ChL6 molecule.

ChL6 Radiolabeling

[111]In-Chloride in 0.05 mol/L HCl (0.4 GBq) was buffered to a final pH of 5.3 in 0.1 mol/L ammonium acetate, and 2IT-BAD-ChL6 (4.0 mg) was added. The solution was incubated for 30 min at 37°C, and then 0.1 mol/L sodium ethylenediaminetetraacetate (EDTA) (Fisher Scientific) was added to a final concentration of 10 mmol/L to scavenge nonspecifically bound [111]In. [111]In-2IT-BAD-ChL6 was purified from ^{111}In-EDTA by molecular-sieving chromatography.

Purified [111]In-2IT-BAD-ChL6 was evaluated by cellulose acetate electrophoresis (CAE), molecular-sieving high-performance liquid chromatography ([HPLC] SEC 3000), and radioimmunoassay using HBT3477 human breast cancer cells (12–15). ^{125}I-ChL6, lightly labeled and previously shown to be indistinguishable from ChL6, was assayed in parallel as a reference standard. HPLC and CAE indicated that 100% and 97%, respectively, of ^{111}In-ChL6 was in monomeric form. The absolute binding in the live cell assays was ≥70% and 100% relative to the ^{125}I-ChL6 reference standard.

Bioprobe Conjugation

A single lot of 20-nm nanoparticles (Nanomag-D-Spio beads) was used for the studies in mice and for the in vitro particle heating measurements. ^{111}In-DOTA-2IT-ChL6 was conjugated with the nanoparticles via amide linkage to the carboxyl (COOH) terminated PEG coating to prepare the ^{111}In-ChL6 bioprobes. For each of 4 preparations, 24.0 mg of EDC and 48 mg of NHS in 10 mL of 0.5 mol/L MES buffer were mixed with 200 mg/12 mL of Spio beads (product-code: 79-56-201). This suspension was incubated for 1 h at room temperature (RT) with continuous mixing, then placed in 3,400 MWCO dialysis bags, and dialyzed against 4 L of saline for 1 h. ^{111}In-DOTA-2IT-ChL6 (148–185 MBq [4–5 mCi]/3–4 mg/1.5 mL of PBS) suspended in 10 mL of 0.1 mol/L MES buffer, was mixed with the activated dialyzed Spio bead suspension and incubated for 1 h at RT with continuous mixing (6.5×10^{13} molecules of mAb/mg of Spio beads). These conjugated ^{111}In-DOTA-2IT-ChL6-D-Spio beads (32 mL) were again placed in 4 dialysis bags

(3,400 MWCO) (8.0 mL) and dialyzed against 4 L of saline at RT for 1 h. The dialyzed product was mixed with 4.0 mL of 25 mmol/L glycine in PBS at RT (15 min) and then applied to the HGMF column using saline washing buffer to remove the nonbound ^{111}In-DOTA-2IT-ChL6.

The final suspension that was collected from the magnetic column with saline wash after removing it from the magnetic field was brown and yielded bioprobes as ^{111}In-DOTA-2IT-ChL6-D-Spio beads (110–150 mg of beads with 10–15 μg mAb/mg and 370–555 kBq/mg [10–15 μCi/mg]). The concentration of the beads was estimated by ultraviolet/visible spectrophotometry at a wavelength of 492 nm using unconjugated beads as a reference, and protein concentration was estimated at a wavelength of 280 nm. Two microliters of final product were applied to multiple CAE strips for electrophoresis of 11 and 45 min, and the immunoreactivity was evaluated in live cell assay. The CAE at 11 and 45 min showed the monomeric final product of 94%–98% and 91%–97% at 11 and 45 min, respectively. Bioprobes moving more slowly than the monomeric product on CAE represented <3% (0.5–2.9), providing evidence of only minimal bioprobe aggregation. In vitro immunoreactivity, as the percentage of ^{111}In-bioprobes bound to HBT3477 cells determined by methods described earlier (15), was >70% of the reference ^{111}In-ChL6 for the bioprobes used in these studies. The specific activity of the ^{111}In-DOTA-2IT-ChL6 bioprobes for injection after being passed through a 0.22-μm filter with no appreciable loss was 370–555 kBq/mg (10–15 μCi/mg).

Mouse Studies

Female (7–9 wk old), athymic Balb/c *nu/nu* mice (Harlan Sprague–Dawley, Inc.) were maintained according to the University of California animal care guidelines on a normal diet ad libitum and under pathogen-free conditions. HBT3477 cells were harvested in logarithmic phase; 3.0×10^6 cells were injected subcutaneously on both sides of the abdomen of mice in the PK study and on only the right side of the abdomen of mice in the Rx study. Two additional mice received subcutaneous injections of HBT3477 cells in 4 sites, 2 on each side. These tumors were harvested for study by EM after AMF Rx.

All studies were initiated 2–4 wk after implantation when the mean tumor volume was 238 ± 32 mm³. PK and Rx studies were performed using ^{111}In-ChL6 bioprobe doses of 740–1,110 kBq (20–30 μCi) on 2.25 mg of bioprobe in 200–300 μL saline, injected intravenously into a lateral tail vein with an additional 50 μg ChL6.

PK Study

PK studies were performed at 1, 2, 3, and 5 d after injection using 5 mice at each time point. ^{111}In-ChL6 bioprobe doses were injected intravenously in 200–300 μL saline. Whole-body activity was measured in a dose calibrator (CRC-12; Capintec, Inc.) immediately and again at 1 and 4 h and 1, 2, 3, and 5 d to the time of sacrifice. Values were expressed as a percentage of injected dose (%ID). Blood activity, expressed as %ID/mL, was determined by counting 2-μL blood samples, collected at 5 min, 1 and 4 h, and 1, 2, 3, and 5 d after injection in a γ-well counter (Pharmacia LKB). The mice were sacrificed and organs and tissue samples were collected. Activity, expressed as %ID/g, was measured in a γ-well counter in a manner similar to that used for blood activity (16).

Therapy Study

Treatment was defined as the administration of AMF 3 d after injection of bioprobes intravenously For Rx studies, mice were divided into 5 groups, 1 group of 9 or 10 mice for each of 5 different AMF applications. Three control groups were used: no AMF or bioprobes (n = 24). bioprobes only with no AMF (n = 5), and AMF only with no bioprobes (n = 5).

AMF was applied 3 d after bioprobe injection; this was defined as the treatment day and used to determine tumor doubling, tripling, and quadrupling times in days (6). At that time, each mouse was anesthetized by injecting 0.02 mL intraperitoneally per gram body weight of a solution prepared by dissolving 0.5 g of 2,2,2-tribromoethanol in 1.0 mL of warm *t*-amyl alcohol, diluting the solution with 40 mL distilled water, and filtering the solution through a 0.2-μm filter.

After the mouse was anesthetized, 3 fiber optic temperature probes (FISO, Inc.) were used to track normal tissue temperatures. One was inserted in the subcutaneum over the lower spine by inserting a 16 gauge × 1½ in. hypodermic needle at the base of the tail and threading the fiber optic probe through the needle under the skin. A second probe was taped onto the skin of a hind limb using a wound dressing, and a third probe was inserted 1 cm into the rectum. After the probes were in place, the mouse was wrapped lightly in absorbent paper and inserted into a 50-mL centrifuge tube with the bottom removed. The tube was inserted into the felt-lined AMF coil, so that the abdominal tumor of the mouse was positioned in the high-amplitude region (1 cm) of the induction coil (Fig. 2). Once the mouse was in place and the parameters were programmed into the controls, the AMF generator was turned on.

Using results from our previous studies, AMF parameters—that is, amplitude, duration, and duty—were selected to minimize nonspecific tissue heating while providing sufficient AMF energy to activate bioprobes in the tumor (6,17). The magnetic field and time parameters sampled in this study are summarized in Table 1. Total duration of AMF treatment in all treatments was 20 min, including both on and off times. After treatment, each mouse was left in the coil until the core (rectal) temperature began to fall; then all probes were removed. The mouse was removed from the coil and centrifuge tube and placed on a warm recovery pad on its back. When the righting reflex returned, the mouse was returned to its cage.

Temperatures were recorded at 1-s intervals for each probe, beginning after each mouse was positioned in the coil, 30 s before AMF treatment. All mice placed in the coil exhibited decreasing temperature (hypothermia) before initiation of AMF treatment, likely due to the combination of anesthesia and the temperature (14°C) of the coil (17). Temperature data were not corrected for this decrease, but maximum rectal, skin, and spine temperatures were recorded and averaged for all mice; the means are reported in Table 2.

Concurrent with the Rx studies, 6 mice underwent a 48-h PK study, 3 mice with each of the 2 staggered Rx groups, temporally offset by 1 d. Data were analyzed to determine whether tumor uptake warranted AMF Rx of the mice in each group. Uptake per gram of tumor was also used to calculate total heat expected from AMF application (see Dosimetry).

EM Studies

Three tumors from PK 24 h after injection and 4 tumors after Rx (2 at 24 and 48 h after AMF [1,300 oersteds [Oe] (104 kA/m), 60% duty]) were placed in Karnovsky's fixative for EM analysis. They were then fixed in osmium tetroxide and embedded in an
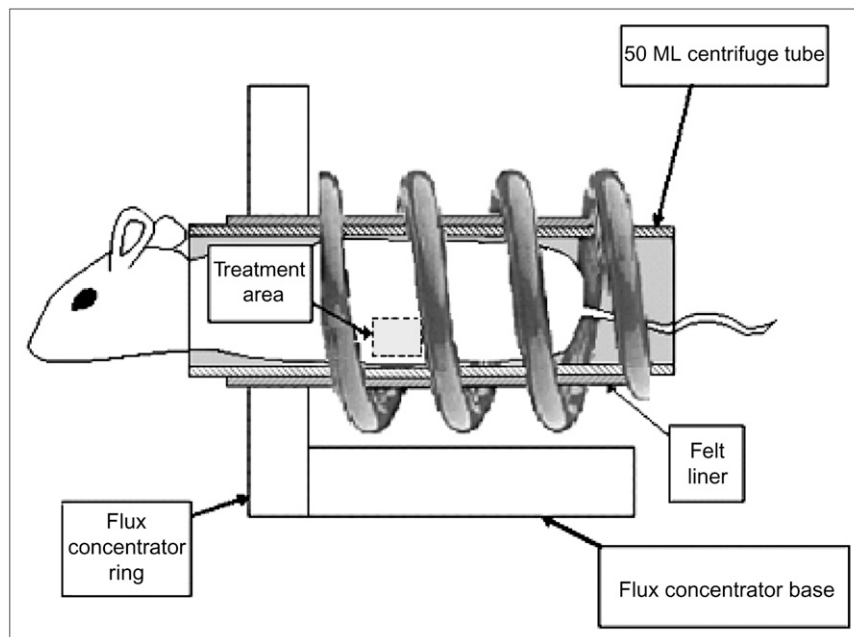
FIGURE 2. AMF delivery coil used to treat mice bearing human xenograft tumors. AMF is focused in a 1-cm band in which subcutaneous tumor located on abdomen of each mouse was positioned. Major components of the system are (a) induction coil, (b) capacitance network, and (c) power supply (*17*).

epoxy resin using standard protocols (*18*). Ultrathin sections were viewed on a Philips CM 120 Biotwin.

Dosimetry

The THD in the tumors in joules per gram (J/g) was calculated using the measured specific absorption rate (SAR) of the iron (Fe) particles at each AMF amplitude studied and a mean bioprobe concentration in the tumors of 14 %ID/g. THD thus is:

$$THD = (M) \cdot (SAR) \cdot (D) \cdot (1,200\,s),$$

where M is the mass concentration of bioprobes in the tumor (grams bioprobes/grams tumor) obtained from the total bioprobe dose injected (2.2 mg) and the mean bioprobe concentration in tumor; *SAR* is the measured heating rate (W/g particles) of the particles as a function of AMF amplitude; *D*, duty, is the fraction of all AMF pulse "on" time over the total treatment time (Table 1); and 1,200 s is the total treatment time of 20 min.

Toxicity and Tumor Response

Toxicity and tumor response were evaluated for all groups of mice by monitoring blood counts (red blood cells [RBC], white blood cells [WBC], platelets [PLT]) 3 times per week for 3 wk and tumor volume and body weight 3 times per week for 12 wk. Blood samples were collected from tail veins using 2-μL microcapillary pipettes. Samples from mice within a treatment group were pooled and diluted 1:200 in PBS (0.9% saline and 10 mmol/L sodium phosphate, pH 7.6) for RBC counts, 1:100 in 1% (w/v) ammonium oxalate for PLT counts, or 1:20 in 3% (w/v) acetic acid for WBC counts (*19–21*). Using caliper measurements in 3 orthogonal directions, tumor volume was calculated using the formula for a hemiellipsoid (*22*). Initial tumor volume was defined as the volume on the day of AMF treatment. Mean tumor volume after treatment was calculated from actual tumor measurements on that day or from values derived from linear interpolation if that day fell between actual measuring days for a mouse in the same treatment group. Tumor growth delay was evaluated for treated mice and

TABLE 1
AMF Treatment Parameters

Group	Amplitude Oe (kA/m)	Duty (%)	Pulse (s)	SAR*	THD†
1	1,410 (113)	30	90	78	9
2	1,050 (84)	50	90	71	13
3	1,050 (84)	70	90	71	19
4	700 (56)	90	90	62	21
5	1,300 (104)	60	120	78	18
Control 1‡	NA	NA	NA	NA	NA
Control 2‡	NA	NA	NA	NA	NA
Control 3‡	1,050 (84)	70	90	0	NA

*Specific absorption rate (SAR) of particles (W/g particles).
†Calculated THD deposited in tumor (J/g tumor).
‡Control groups 1, 2, and 3 received nothing, bioprobes without AMF, and AMF without bioprobes, respectively.
NA = not applicable.

TABLE 2
Maximum Temperature (°C) Response to AMF Measured In Vivo (Mean ± SE)

Group	Rectal	Skin	Spine
1	37.1 ± 0.3	39.7 ± 0.7	35.4 ± 0.3
2	35.9 ± 0.4	37.5 ± 0.5	37.0 ± 0.4
3	38.7 ± 0.3	41.0 ± 0.3	39.7 ± 0.3
4	34.4 ± 0.3	34.7 ± 0.4	34.6 ± 0.2
5	43.0 ± 0.4	45.6 ± 0.4	44.4 ± 0.4
Control 3*	37.2 ± 0.3	40.1 ± 0.3	39.0 ± 0.7

*Group of mice receiving AMF but no bioprobes.

mice receiving no treatment. Mice dying before 30 d from toxicity were excluded from tumor response results.

Tumor effects were analyzed by Wilcoxon rank sum comparison of the time to double, triple, and quadruple tumor volume. The growth rates for the AMF-only and bioprobe-only control groups were compared with the untreated (no AMF or bioprobes) group and with each other and were not significantly different from each other. They were, therefore, combined as the control for comparisons with the treatment groups. Doubling, tripling, and quadrupling times for each treated group and the combined treatment groups were compared with that of the control group. Comparisons were also made of each treated group with all other treated groups. The 1,050-Oe (84 kA/m) groups treated at 50% and 70% duty (13 and 19 J/g tumor) were indistinguishable (doubling, tripling, and quadrupling $P = 0.8, 0.3,$ and 0.5, respectively); they were, therefore, combined and compared with controls as the 1,050-Oe (84 kA/m) group.

AMF System

The AMF system used to treat the xenografts was designed and built to provide high-amplitude AMF in an approximately 1-cm band to the lower abdomen of a mouse. The system and its design have been previously described (17). Briefly, the system consisted of 3 main components: (a) the induction coil, or inductor; (b) a capacitance network that, when combined with the inductor, forms a resonant circuit; and (c) the power supply. The length of the induction coil was 40 mm with an internal diameter of 36 mm, which enabled insertion of a 50-mL conical centrifuge tube containing a mouse and allowing for 2.5 mm of thermal insulation around the circumference of the 50-mL tube (Fig. 2). It was manufactured from square cross-sectional oxygen-free, high-conductivity copper tubing and included a low-reluctance flux-concentrating ring made of Fluxtrol 50 (Fluxtrol) on the end of the solenoid coil to divert magnetic flux away from areas not intended to receive high-amplitude AMF treatment. This provided a preferential path for the magnetic flux to the interior of the solenoid, producing an approximately 1-cm band of high-amplitude AMF for tumor treatment.

The field amplitude across the 1-cm band was measured before each set of trials and for each generator power setting used, ensuring that this field gradient (variation of amplitude) in the tumor treatment area was within 2% at Oe $\leq$ 1,210 Oe and well within 6% at the maximum oersteds used. It is the amplitude within this region that is reported as AMF amplitude. During operation, the induction coil itself heats and was cooled using a closed-loop circulating water system maintained at 14°C $\pm$ 2°C during operation. The capacitance network was built into the power supply and was adjusted for stable oscillation at 153.0 $\pm$ 0.5 kHz. A pulse-timer circuit (manufactured by Giltron, Inc.) was installed, allowing 0.5- to 9,999-s pulses at any duty (0%–100%).

Particle SAR Measurements for Dosimetry Calculations

In vitro particle heating SAR measurements were performed using another AMF system configured with an appropriate helical coil designed to accommodate a suitable calorimeter. The AMF system used for particle SAR measurements also operated at a resonant frequency of 153.0 $\pm$ 0.5 kHz, and the peak AMF amplitude at the center of the coil was adjustable to between 300 and 1,600 Oe. The apparatus was calibrated with a magnetic probe, and the magnetic field amplitudes versus the percentage drive voltage were plotted, ensuring a homogeneous field in the area of the sample placement.

One-milliliter aliquots of sample bioprobe suspensions were heated in the coil by AMF at various amplitudes, and temperatures

were measured and recorded using fiber optic probes as described. Temperature was recorded 1–10 times per second for each sample and at each AMF setting. The process was repeated using buffer (water) blanks—that is, no particles—to correct for heat losses of the calorimeter. Heat produced (in W/g particle) was calculated for each AMF amplitude setting from the slope of the net temperature rise (°C/s) using the heat capacity of 1 mL of pure water (4.18 J/g °C) and normalized for the concentration of particles in the sample. Measured SAR values at the AMF for specific study groups are reported in Table 1.

RESULTS

Pharmacokinetics

Blood and body clearances of the ^{111}In-ChL6 bioprobes compared with ^{111}In-ChL6 are shown in Figure 3A. Mean ^{111}In-ChL6 bioprobe concentrations (%ID/g) in lung,
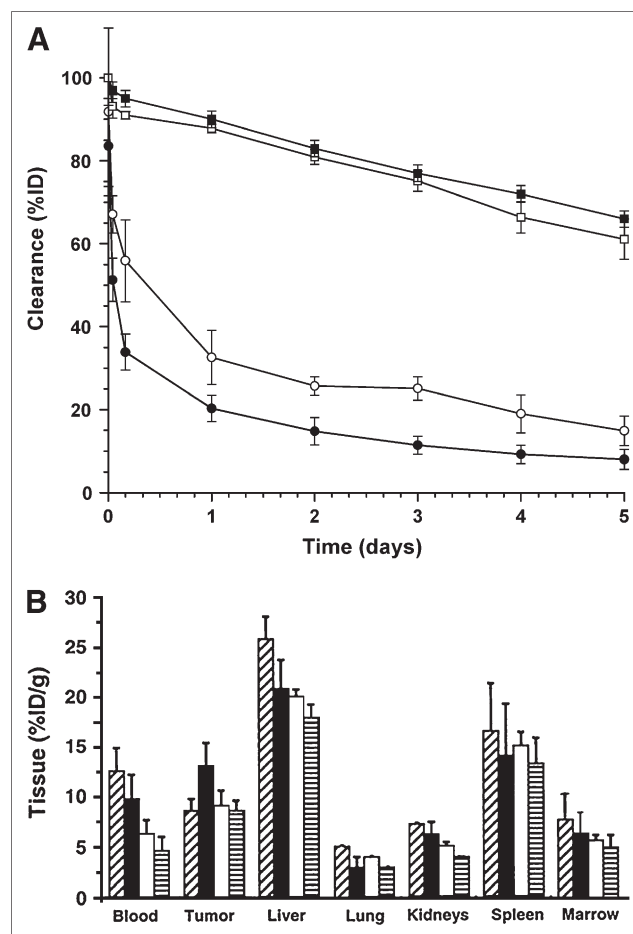
FIGURE 3. Pharmacokinetics of ^{111}In-ChL6 bioprobes in mice with HBT3477 human breast cancer xenografts. (A) Blood clearance of ^{111}In-ChL6 bioprobes (●) was more rapid than that of ^{111}In-ChL6 mAb alone (○). Whole-body clearances (■, □) were similar. (B) Concentrations (%ID/g) of ^{111}In-ChL6 bioprobes in blood, tumor, liver, lung, kidneys, spleen, and marrow at 1 d (▨), 2 d (■), 3 d (□), and 4 d (▤) after injection. Maximum concentrations in liver and spleen were almost twice and tumor concentration was about 75% of that previously observed for ^{111}In-ChL6 mAb (16). Concentrations of ^{111}In in other normal tissues were similar to those of ^{111}In-ChL6 mAb.

kidney, and marrow (Fig. 3B) were similar to those of ^{111}In-ChL6 alone as previously reported (16), whereas liver and spleen concentrations were twice that of ^{111}In-ChL6. Tumor mean concentrations of ^{111}In-ChL6 bioprobes in the PK study were between 9.7 and 13.7 %ID/g and were considered to be constant (not significantly different) over the 5-d study. PK at 48 h after injection in 6 mice studied in parallel with the Rx study demonstrated mean tumor concentrations of 14 ± 2 %ID/g.

Toxicity

All treated mice demonstrated no particle-related toxicity and no toxicity for the Rx with the exception of mice in group 5 (Table 1). Groups 1–4 had blood counts, weights, and appearances similar to those of untreated mice, and temperature data from these groups suggested that toxicity should not be expected (Table 2).

Group 5 mice treated with 1,300 Oe (104 kA/m) at 60% duty and 120-s pulse "on" time had 6 deaths within 24 h of AMF. This group of mice received AMF with the longest pulse time in the study. Mean rectal (43.0°C $\pm$ 0.4°C), skin (45.6°C $\pm$ 0.4°C), and spinal (44.4°C $\pm$ 0.4°C) temperatures were the highest of all groups of mice, suggesting that nonspecific heating from eddy current production resulted in the observed toxicity as described in a previous study with nontumor mice and no bioprobes (17). The 4 surviving mice in this group demonstrated acute skin changes manifested by denuded and erythematous area and did not represent an adequate number of surviving mice for inclusion in the tumor response analysis.

Tumor Response

Tumor growth delay as the indicator of response was used to compare treated and control mice, as described (Table 3; Fig. 4). There was a significant increase in doubling, tripling, and quadrupling times of tumors in treated groups of mice compared with the nontreated control group and with the combined control group of mice except for tumors in group 1 that received a substantially lower THD than the other treated groups.

Table 1 shows the calculated tumor THD from the 20-min AMF treatment. The THD calculated for 1,410 Oe (113 kA/m) at 30% duty was 9 J/g, whereas 1,050 Oe (84 kA/m) at 50% and 70% duty gave 13 and 19 J/g, respectively, and 700 Oe (56 kA/m) at 90% duty resulted in 21 J/g tumor. Tumors receiving 1,050 Oe (84 kA/m) at 50% and 70% duty (THDs of 13 and 19 J) showed no difference in tumor doubling, tripling, or quadrupling times (Wilcoxon rank sum $P = 0.8, 0.3,$ and $0.5,$ respectively) and were combined for further analysis. Control tumor growth (no treatment) was compared with both the bioprobe-only and the AMF-only tumor growth groups; no significant differences were observed. The correlation of the calculated total THD with tumor growth rate was therefore evaluated by comparing the response of 3 groups with the untreated controls: THDs of 9 J, 13–19 J, and 21 J. Tumors receiving

TABLE 3
Wilcoxon Rank Sum Comparisons of Tumor Doubling, Tripling, and Quadrupling Times for Treatment vs. Control Groups of Mice

Joules	n	Mean $\pm$ SD	2-sided P
Doubling times			
9	10	10.5 $\pm$ 3.3	0.12
13–19	19	19.0 $\pm$ 22.7	0.01
21	9	20.0 $\pm$ 23.0	0.03
All treated	38	17.0 $\pm$ 20.0	0.004
Controls	34	11.5 $\pm$ 16.2	NA
Tripling times			
9	10	17.6 $\pm$ 5.4	0.12
13–19	19	24.6 $\pm$ 21.1	0.02
21	9	30.2 $\pm$ 20.2	0.007
All treated	38	24.1 $\pm$ 18.6	0.004
Controls	34	18.7 $\pm$ 21.2	NA
Quadrupling times			
9	10	28.3 $\pm$ 19.3	0.11
13–19	19	29.9 $\pm$ 20.0	0.03
21	9	36.2 $\pm$ 18.8	0.005
All treated	38	31.0 $\pm$ 19.7	0.004
Controls	34	22.7 $\pm$ 20.3	NA

NA = not applicable.

13–19 and 21 J showed a measurable and significant tumor growth delay in response to heat dose (Fig. 4; Table 3).

EM

Two tumors were harvested from mice 48 h after intravenous injection of ^{111}In-ChL6 bioprobes (no AMF) and 4
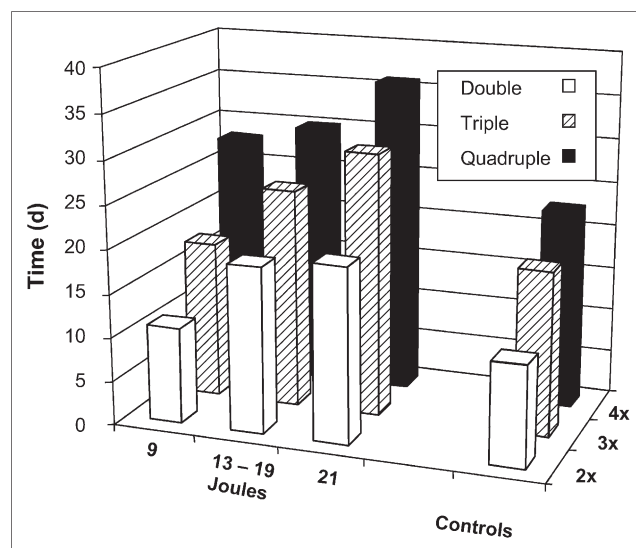
FIGURE 4. Relationship of tumor response to bioprobe AMF Rx. Therapeutic response is reflected by increased time to double, triple, and quadruple tumor volume in mice receiving higher THDs (J). A statistical relationship between response and THD was demonstrated for tumors receiving 13–19 and 21 J/g compared with that of controls (Table 3). Tumor growths of AMF alone, bioprobes alone, and untreated control groups of mice were statistically indistinguishable, so they were grouped as controls.

tumors were harvested after bioprobes followed by AMF (2 each at 24 and 48 h, respectively). The calculated THD delivered to the AMF-treated tumors was 18 J/g. PK tumors showed easily detectable bioprobes on the tumor cells (data not shown) and a healthy appearance of the cells (Fig. 5A). Tumors taken after treatment demonstrated many patchy areas of tumor cell necrosis. There was marked evidence of progressive tumor cell necrosis between 24 h (Fig. 5B) and 48 h (Fig. 5C) after AMF.

DISCUSSION

Thermal ablation has been considered as a therapeutic modality for cancer (3,4). The inability to safely induce a therapeutic response because of difficulties in inducing selective tumor heating and facilitating heat dose have limited its widespread use in clinical Rx. The approach for cancer thermal ablation presented here combines tumor cell immunotargeted magnetic nanoparticles and cytotoxic heat from their response to externally applied AMF. The use of radiolabeled bioprobes facilitated quantitation of tumor concentrations of bioprobes and the calculation of tumor heat dosimetry that correlated with observed tumor growth delay in xenografts.

This study demonstrates that bioprobes can be produced with ^{111}In-ChL6 linked to 20-nm iron dextran nanoparticles that target human breast cancer xenografts in mice. Compared with published information for various nanoparticles

FIGURE 5. Electron micrographs of ultrathin osmium tetroxide–fixed epoxy-embedded HBT3477 xenografts that had been excised from mice at time of sacrifice: (A) 48 h after bioprobes, no AMF; (B) 24 h after AMF Rx (18 J/g); and (C) 48 h after AMF Rx (18 J/g). Healthy cells (A) contrast with evidence for cell necrosis at 24 h after AMF Rx (B) and further evidence for necrosis 48 h after AMF Rx (C).

(23,24), these ^{111}In-ChL6 bioprobes remained in the circulation sufficiently long, albeit shorter than ^{111}In-ChL6 mAb (16), to allow significant tumor accumulation. The presence of the bioprobes in the tumor xenografts was confirmed by quantitation of tumor radiotracer in the PK study and by EM demonstration of iron nanoparticles in the tumors.

The potential of this Rx was demonstrated in an aggressive human breast cancer xenograft model. Treated tumors, having bioprobes activated by AMF, demonstrated tumor growth rate delay; this tumor response correlated with the calculated heat dose delivered. Tumor growth rates for mice receiving external AMF or bioprobes alone were not statistically different from those of the control group of mice that received neither AMF nor bioprobes.

The lowest AMF amplitude (Oe) and highest duty ("on" time) combination—that is, 700 Oe (56 kA/m) and 90% duty—that was tested delivered safely the highest calculated THD and was associated with the greatest therapeutic effect on the tumors. Particle heat output, or SAR, is a function of AMF field amplitude (Table 1). However, high amplitudes at this frequency also deposit more nonspecific heat to normal tissues from increased eddy current production (Table 2) (17). To prevent overheating in normal tissues, the duty must be reduced at these higher amplitudes, providing greater "off" time between pulses for heat to dissipate. By contrast, lower-amplitude AMF can be sustained with little "off" time without compromising safety as the nonspecific heat that is generated in normal tissue does not challenge normal mechanisms that dissipate heat. Consequently, the THD to the tumor can be safety enhanced because the particles generate heat for a greater percentage of the total treatment time despite the decreased SAR. The result is a greater net heat deposited to the tumor and less heat deposited to surrounding tissues. Further study of heat dosimetry and the effect of further reduction of AMF amplitude while maintaining THD is warranted (Table 2).

Tumor responses of the study groups evidenced heat dose dependence and thermal dosimetry relevance to THD, a conceptual parallel to radiation dosimetry. Quantitative imaging studies may provide a prescription-based approach for this AMF therapeutic modality. Nanoparticles have recently been developed with 5–10 times the heat response to AMF compared with the bioprobes that were used in this study. Thus, predictive dosimetry derived from their bioprobe PK and tumor uptake may offer further insights into the success of clinical translation of this modality. Furthermore, thermal Rx could be combined with radioisotope Rx using a different radionuclide for labeled nanoparticles or in series with external beam radiation Rx.

It is noteworthy that the tumor response, when detectable on EM, was cell death by necrosis that progressed with time after treatment. Surprisingly, although apoptotic changes in dying cells are quite well recognized by EM, almost no tumor cells were seen undergoing apoptosis in

these treated tumors. Nonhomogeneity of the effect was evident and most likely related to inhomogeneous delivery of the bioprobes, similar to the situation in radioimmunotherapy. Improvement in the homogeneity of bioprobe distribution in tumor tissue may be achieved by fractionation of the ID (*25*); the effects of multiple doses on homogeneity of bioprobes in tumor could be demonstrated by future studies using autoradiography of serial tumor samples. Such an approach to Rx is practical because of the stability of bioprobe concentrations in tumor over time before AMF application.

CONCLUSION

This study suggests that a modality for delivering thermoablation to cancer cells is feasible. Tumor response with evidence of heat dose dependence was achieved without toxicity. Tumor concentrations of systemically injected ^{111}In-bioprobes and the resulting calculated heat dosimetry for AMF application levels were predictive of tumor response. This thermal dosimetry system represents a concept analogous to that of radiation dosimetry for radiotherapy. As in radioimmunotherapy, this approach may assist in the safe and effective development of this new thermal modality. Significant results include successful bioprobe formulation resulting in effective tumor targeting; tumor responses without normal tissue toxicity that were statistically validated; calculated tumor heat dose correlated with response; and calculated heat dose to tumor versus normal tissue from AMF pulse, permitting increased THD without toxicity.

REFERENCES

1. Overgaard J. History and heritage: an introduction. In: Overgaard J, ed. *Hyperthermia Oncology*. London, U.K.: Taylor and Francis; 1985.
2. Streffer C, van Beuningen D. The biological basis for tumor therapy by hyperthermia and radiation. In: Streffer J, ed. *Hyperthermia and the Therapy of Malignant Tumors*. Berlin, Germany: Springer; 1987:24–70.
3. Hildebrandt B, Wust P, Ahlers O, et al. The cellular and molecular basis for hyperthermia. *Crit Rev Oncol Hematol*. 2002;43:33–56.
4. Moroz P, Jones SK, Gray BN. Magnetically mediated hyperthermia: current status and future directions. *Int J Hyperthermia*. 2002;18:267–284.
5. Dewhirst MW, Jones E, Samulski T, Vujaskovic Z, Li C, Prosnitz L. Hyperthermia. In: Kufe D, Pollock R, Weichselbaum R, et al., eds. *Cancer Medicine*. Hamilton, Ontario, Canada: BC Decker, Inc.; 2003:623–636.
6. DeNardo SJ, DeNardo GL, Miers LA, et al. Development of tumor targeting bioprobes (^{111}In-chimeric L6 monoclonal antibody nanoparticles) for alternating magnetic field cancer therapy. *Clin Cancer Res*. 2005;11(suppl):7087s–7092s.
7. Fell HP, Gayle MA, Yelton D, et al. Chimeric L6 anti-tumor antibody: genomic construction, expression, and characterization of the antigen binding site. *J Biol Chem*. 1992;267:15552–15558.
8. Liu AY, Robinson RR, Hellstrom KE, Murray EDJ, Chang CP, Hellstrom I. Chimeric mouse-human IgG1 antibody that can mediate lysis of cancer cells. *Proc Natl Acad Sci U S A*. 1987;84:3439–3443.
9. Hellstrom I, Horn D, Linsley P, Brown JP, Brankovan V, Hellstrom KE. Monoclonal antibodies raised against human lung carcinomas. *Cancer Res*. 1986;46:3917–3923.
10. Marken JS, Bajorath J, Edwards CP, et al. Membrane topology of the L6 antigen and identification of the protein epitope recognized by the L6 monoclonal antibody. *J Biol Chem*. 1994;269:7397–7401.
11. McCall MJ, Diril H, Meares CF. Simplified method for conjugating macrocyclic bifunctional chelating agents to antibodies via 2-iminothiolane. *Bioconjug Chem*. 1990;1:222–226.
12. DeNardo SJ, DeNardo GL, Kukis DL, et al. [67]Cu-2IT-BAT-Lym-1 pharmacokinetics, radiation dosimetry, toxicity and tumor regression in patients with lymphoma. *J Nucl Med*. 1999;40:302–310.
13. Moi MK, Meares CF, DeNardo SJ. The peptide way to macrocyclic bifunctional chelating agents: synthesis of 2-(p-nitrobenzyl)-1,4,7,10-tetraazacyclododecane-N,N′,N″,N‴-tetraacetic acid and study of its yttrium (III) complex. *J Am Chem Soc*. 1988;110:6266–6267.
14. Kukis DL, DeNardo SJ, Mills SL, Shen S, O'Donnell RT, DeNardo GL. Stability of monoclonal antibodies, Lym-1 and ChL6, and 2IT-BAD-Lym-1 immunoconjugate with ultra freezer storage. *Cancer Biother Radiopharm*. 1999;14:363–369.
15. Kukis DL, DeNardo GL, DeNardo SJ, et al. Effect of the extent of chelate substitution on the immunoreactivity and biodistribution of 2IT-BAT-Lym-1 immunoconjugates. *Cancer Res*. 1995;55:878–884.
16. DeNardo SJ, Burke PA, Leigh BR, et al. Neovascular targeting with cyclic RGD peptide (cRGDf-ACHA) to enhance delivery of radioimmunotherapy. *Cancer Biother Radiopharm*. 2000;15:71–79.
17. Ivkov R, DeNardo SJ, Daum W, Foreman A, Goldstein R, DeNardo GL. Application of high amplitude alternating magnetic fields for heat induction of nanoparticles localized in cancer. *Clin Cancer Res*. 2005;11:7093s–7103s.
18. Hayat MA. *Principles and Techniques of Electron Microscopy: Biological Applications*. Boca Raton, FL: CRC Press; 1998.
19. Burke PA, DeNardo SJ, Miers LA, Kukis DL, DeNardo GL. Combined modality radioimmunotherapy: promise and peril. *Clin Cancer Res*. 2002;94(4 suppl): 1320–1331.
20. DeNardo GL, Kukis DL, Shen S, et al. Efficacy and toxicity of [67]Cu-2IT-BAT-Lym-1 radioimmunoconjugate in mice implanted with Burkitt's lymphoma (Raji). *Clin Cancer Res*. 1997;3:71–79.
21. Seiverd C. *Hematology for Medical Technologists*. Philadelphia, PA: Lea and Febiger; 1972:91–432.
22. DeNardo SJ, Kukis DL, Miers LA, et al. Yttrium-90-DOTA-peptide-chimeric L6 radioimmunoconjugate: efficacy and toxicity in mice bearing p53 mutant human breast cancer xenografts. *J Nucl Med*. 1998;39:842–849.
23. DeNardo SJ, Richman CM, Goldstein DS, et al. Yttrium-90/indium-111-DOTA-peptide-chimeric L6: pharmacokinetics, dosimetry and initial results in patients with incurable breast cancer. *Anticancer Res*. 1997;17:1735–1744.
24. Jordan A, Scholz R, Wust P, Fahling H, Felix R. Magnetic fluid hyperthermia (MFH): cancer treatment with AC magnetic field induced excitation of biocompatible superparamagnetic nanoparticles. *J Magnetism Magn Mater*. 1999; 201:413–419.
25. DeNardo GL, Schlom J, Buchsbaum DJ, et al. Rationales, evidence and design considerations in fractionated radioimmunotherapy. *Cancer*. 2002;94: 1332–1348.